



ELSEVIER

Applied Surface Science 184 (2001) 307–316

applied
surface science

www.elsevier.com/locate/apsusc

p-Type doping of SiC by high dose Al implantation—problems and progress

V. Heera^{*}, D. Panknin, W. Skorupa

Forschungszentrum Rossendorf, P.O. Box 510119, D-01314 Dresden, Germany

Abstract

The development of optimized processes for p-type doping of SiC by ion implantation and subsequent annealing is a remaining challenge to SiC-device technology. Al is a promising acceptor in SiC. Compared to B it has a shallower acceptor level and a stronger tendency to occupy atomic sites in the Si sublattice which makes Al more suitable for the production of heavily doped, low resistivity layers. However, also in the case of Al very high acceptor concentrations ($>10^{19} \text{ cm}^{-3}$) are necessary to obtain SiC layers with low resistivities ($<1 \Omega \text{ cm}$). The physical consequences of such high impurity concentrations in SiC for the annealing of implantation damage and the electrical activation will be discussed. A survey of the results of several implantation and annealing schemes is presented. © 2001 Published by Elsevier Science B.V.

Keywords: SiC; p-Type doping; Al implantation; Resistivity; Annealing

1. Introduction

Ion implantation is the only practicable method for selective doping of SiC, because dopant diffusion needs too high temperatures. Whereas N implantation has successfully been applied in order to produce low resistivity, n-type SiC regions, the development of efficient processes for p-type doping is still a challenging task. High dose Al implantation seems to be the most promising procedure to fabricate low resistivity, p-type regions in SiC and, therefore, many experimental studies have been performed in this field in order to find out the optimum conditions for the implantation and the subsequent damage annealing. This paper is an attempt to summarize and assess these results in the context of the underlying physics. The

fundamental limits for the hole generation and the resulting resistivity in heavily Al doped SiC will be discussed in Section 2. It should be emphasized that this will be done on the most simple level and specific effects like slightly different acceptor states in the different polytypes and anisotropic hole conduction will not be considered. Usually, the acceptor activation grade which depends on the processing conditions has been taken as a quality mark of the doping process. It will be demonstrated that the temperature range over which Hall measurements can be performed is much too low to determine reliable values for the acceptor activation in heavily doped SiC. Therefore, it is better to directly compare the measured resistivities with their theoretical limits. Issues related to the Al lattice site occupation, precipitation and compound formation will be specified in Section 3. The problems associated with the damage formation by high dose ion implantation and the efforts to reduce it by elevated implantation temperatures and/or post-implantation

^{*} Corresponding author. Tel.: +49-351-260-3343;
fax: +49-351-260-3411.
E-mail address: heera@fz-rossendorf.de (V. Heera).

annealing will be reported in Section 4. Finally, the results of different doping schemes will be compared with the theoretical limits for the resistivities and conclusions for optimum doping conditions will be drawn.

2. Acceptor ionization and resistivity—physical limits

The resistivity ρ of p-type SiC is given by

$$\rho = \frac{1}{pe\mu} \quad (1)$$

where p , e and μ are the concentration of holes in the valence band, the electron charge and their mobility, respectively. In order to understand the problems associated with the production of low resistivity, p-type SiC, we have to consider first the physical limits of the hole generation. The ionization energies of acceptor atoms for SiC are listed in Table 1. Unfortunately, the acceptor levels in SiC are much deeper than in Si which makes it very difficult to achieve high hole concentrations p as follows from the neutrality condition [1]

$$p + N_D = \frac{N_A}{1 + p/x} \quad (2)$$

in which N_A and N_D are the concentrations of acceptors and compensating donors, respectively. The parameter x depends on the temperature and includes the density of states of the valence band, the acceptor degeneracy factor and the acceptor ionization energy E_A . For SiC [2], it is about

$$x = 1.2 \times 10^{15} \text{ cm}^{-3} \text{ K}^{-3/2} T^{3/2} \exp\left(-\frac{E_A}{kT}\right) \quad (3)$$

Table 1

Ionization energies E_A of acceptor atoms in the 6H- and 4H-polytype of SiC. Experimental results vary in dependence on the measurement methods, doping concentration and lattice site symmetry [1]. The corresponding values for acceptor atoms in Si are shown for comparison

	E_A (meV), Al	E_A (meV), B	E_A (meV), Ga
6H-SiC	200–250	300–400	317–333
4H-SiC	191–230	285–390	267
Si	57	45	65

The following limits for the solution of Eq. (2) are of interest:

1. Freeze-out range, high compensation:

$$x \ll \frac{N_D^2}{N_A - N_D} \Rightarrow p = x \frac{N_A - N_D}{N_D} \sim T^{3/2} \times \exp\left(-\frac{E_A}{kT}\right) \quad (4)$$

2. Freeze-out range, weak compensation:

$$\frac{N_D^2}{N_A - N_D} \ll x \ll N_A - N_D \Rightarrow p = [x(N_A - N_D)]^{1/2} \sim T^{3/4} \exp\left(-\frac{E_A}{2kT}\right) \quad (5)$$

3. Saturation range:

$$x \gg N_A - N_D \Rightarrow p = N_A - N_D \quad (6)$$

In Fig. 1, the room temperature (RT) ionization grade $I = p/N_A$ of B and Al is shown for uncompensated SiC as a function of the acceptor concentration. For comparison, the ionization behavior of B in Si is given, too. In contrast to Si, incomplete acceptor ionization is the standard situation in SiC at RT. Obviously, the high ionization energies are responsible for this adverse behavior. For high doping concentrations ($N_A \gg x$), the ionization grade behaves like $I \sim (1/N_A)^{1/2}$ (see Eq. (5)) and, therefore, heavy doping is not very efficient. In practice, the hole concentrations obtained for a given Al concentration N_A^* is even lower than $p = IN_A^*$ because only a fraction $A = N_A/N_A^*$ of the Al atoms occupy Si sites in the SiC lattice where they form the shallow acceptor states. Additionally, active acceptors can be partly compensated by donors. Traditionally, the activation grade A is used as a quality mark of the doping process because it depends sensitively on the processing conditions. Usually, doped semiconductors are characterized by Hall and SIMS measurements in order to determine p and N_A^* , respectively. Then, the activation grade can be calculated via $A = p/(IN_A^*)$. This procedure is straightforward if the temperature during the Hall measurements is high enough for almost complete ionization ($I \approx 1$). Unfortunately, the temperatures necessary to approach the saturation range ($x \gg N_A$) in heavily Al doped SiC are much too high as illustrated in Fig. 2, where the parameter x is plotted as function of the temperature (Eq. (3)). In order to obtain $x = N_A$ for an Al concentration of $1 \times 10^{19} \text{ cm}^{-3}$, the

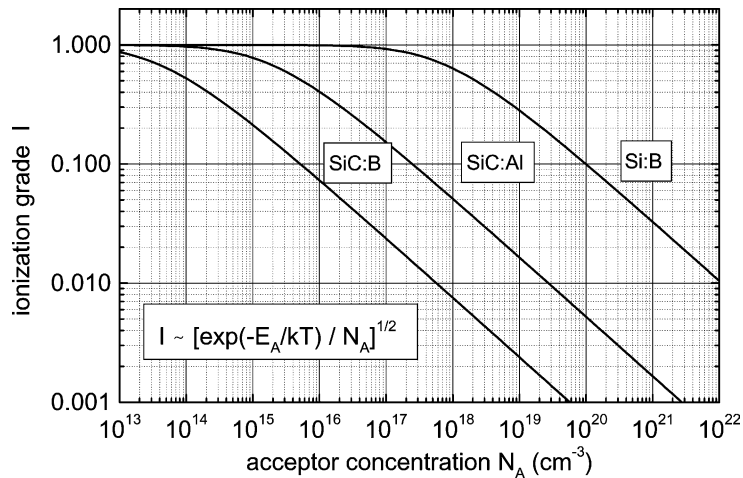


Fig. 1. The ionization grade I of uncompensated SiC at RT as function of the Al and B acceptor concentration in SiC calculated for typical ionization energies of 200 and 300 meV, respectively. The ionization grade of B (45 meV) in Si is shown for comparison. The formula in the inset describes the asymptotical behavior of the ionization grade.

temperature must be raised to about 1000 °C. The ionization grade at this temperature is $I = 0.62$. For an ionization grade $I > 0.9$ the temperature must be even higher than 2500 °C. It should be emphasized that the typical temperature range of Hall measurements (−190 to 600 °C) is much too narrow in order to obtain reliable result for N_A and N_D in heavily p-type doped SiC. Moreover, the common way to plot $\ln(p)$ over $1/T$ in order to determine the ionization energy yields values anywhere between $\frac{1}{2}E_A$ and E_A in

dependence of compensation and temperature (see Eqs. (4) and (5)). Consequently, many of the activation results presented in the literature are not very reliable.

In order to evaluate the quality of doping by implantation and subsequent annealing it seems much more reasonable to compare resistivities because the radiation damage influences the acceptor activation as well as the hole mobility. The highest mobility values have been obtained for in situ doping during epitaxial regrowth [3]. Using these values and the hole concentration of

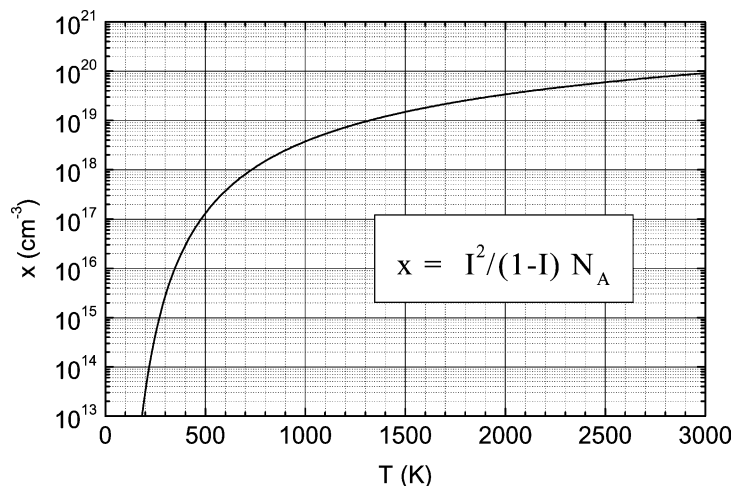


Fig. 2. The parameter x (see Eqs. (3)–(6)) for Al in SiC as function of temperature. The value of x which is necessary to obtain a certain ionization grade I in uncompensated SiC with an Al concentration N_A is determined by the formula given in the inset.

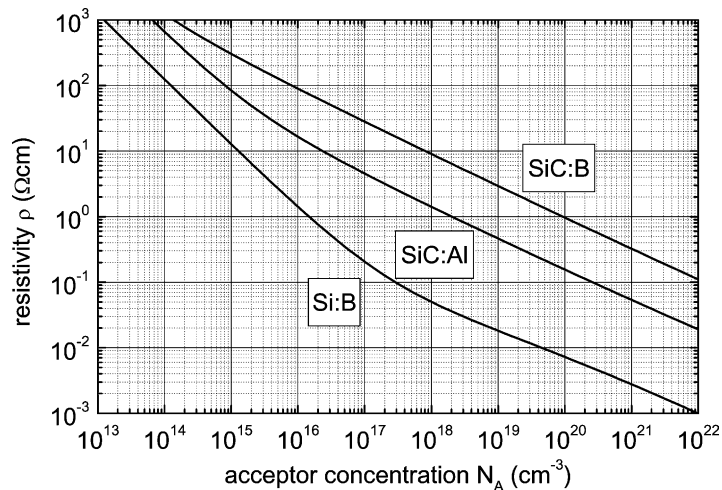


Fig. 3. Predicted minimum resistivity (complete acceptor activation, no compensation, epilayer mobilities) at RT for normal band conduction (no acceptor interaction) as a function of the acceptor concentration.

uncompensated material, the minimum resistivity can be calculated via Eq. (1). The minimum RT resistivities of Si:B, SiC:Al and SiC:B are shown as a function of the acceptor concentration in Fig. 3.

Due to the inefficient hole generation process, very high Al concentrations are necessary to produce low resistivity p-type SiC. However, such high concentrations give rise to new problems. The acceptors can be passivated by precipitation and defect states in the heavily damaged material. The growing number of lattice defects leads to a dramatic drop in the hole mobility. On the other hand, the hole generation can be facilitated by changes in the electronic structure of the heavily doped SiC. It was demonstrated by Schöner et al. [4] that the ionization energy of the Al acceptors decreases with increasing concentration if the compensation grade is higher than 0.01. For acceptor concentrations above $1 \times 10^{21} \text{ cm}^{-3}$, an acceptor band is formed which can lead to metallic conduction if the lattice damage is low enough. Otherwise hopping conduction can be expected as often observed in amorphous semiconductors or ceramics [5].

3. Lattice site occupation, precipitation and phase formation

As mentioned above, group III atoms act as shallow acceptors only if they occupy Si sites in the SiC lattice.

Therefore, efficient p-type doping requires acceptor atoms which have a natural tendency to substitute the Si atoms in the SiC compound. Fortunately, Al fulfills this requirement in a nearly ideal manner, because in contrast to B only the replacement of Si by Al is energetically favorable as demonstrated by tight-binding calculations (Table 2) [6]. Two additional advantages of the Al acceptor are connected with its physical similarity to Si. The similar atomic size prevents large lattice distortions which could act as scattering centers or even traps for the holes. Moreover, the almost equal masses facilitate the direct replacement of Si by Al in atomic collisions during ion implantation doping. The preferential substitution of Si by Al has directly been observed by atomic depth profiling of SiC implanted with very high doses of Al ($c_{\text{Al}} > 1 \text{ at.}\%$) [7]. The Si profile appears as the mirror image of the Al profile, whereas the C profile does not change as long as no new phase has been formed.

There have been several attempts to enhance the acceptor activation by co-implantation of C [8–12].

Table 2
Calculated binding energies of Al and B on Si or C sites in SiC [6]

	Binding energy (eV) on Si site	Binding energy (eV) on C site
Al	2.39	-7.93
B	10.63	11.14

The idea behind is that the presence of C excess atoms in SiC decreases the number of C vacancies and, therefore, increases the probability that the acceptor atoms occupy Si vacancies. An activation enhancement up to a factor of 3 has been found after C co-implantation. In order to obtain optimum results the C implantation must be carried out at elevated temperatures and should not exceed a concentration of $1 \times 10^{18} \text{ cm}^{-3}$. Most probably, this is a consequence of the disorder-stabilizing effect of C in SiC. The implantation sequence as well as the temperature of the Al implantation seems to be of minor importance for the activation process in this concentration range as demonstrated by Ohshima et al. [12]. Obviously, the effects of C co-implantation become more complex than predicted by the simple site competition model if the Al concentration is higher than $1 \times 10^{19} \text{ cm}^{-3}$. A deterioration of the Al activation is observed after C implantation in SiC doped with $1 \times 10^{20} \text{ cm}^{-3}$ Al [8]. In contrast, Tone and Zhao [10] as well as Bluet et al. [11] reported about improved sheet conductivities and lowered contact resistances after C/Al implantations in the dose range between 1×10^{20} and $1 \times 10^{21} \text{ cm}^{-3}$. However, this improvement is due to impurity band conduction as indicated by the temperature dependence of the sheet conductivity. It has frequently been observed that predamaged SiC surfaces form better contacts. Therefore, it is not surprising that the lowest contact resistance has been obtained for RT implantation which produces amorphous layers.

Activation problems can appear if the acceptor concentration exceeds the solubility limit in SiC. The solubility limits of dopants in 6H-SiC grown by sublimation on the C or Si face at temperatures between 2000 and 2400 °C have been investigated by Vodakov et al. [13]. The values obtained for 2000 °C are $9 \times 10^{19}/7 \times 10^{20} \text{ cm}^{-3}$ (C/Si face) for Al and $3 \times 10^{19}/5 \times 10^{19} \text{ cm}^{-3}$ (C/Si face) for B. It should be emphasized that also in this respect Al is superior to B. Linnarson et al. [14] have recently determined the solubility limit of Al in epitaxially grown, heavily doped 4H-SiC layers by the analysis of structural and compositional changes after annealing in the temperature range between 1700 and 2000 °C. It has been found that the solubility limit of Al is about $2 \times 10^{20} \text{ cm}^{-3}$ in the investigated temperature range. Above this critical concentration the formation of Al containing precipitates has been observed after

annealing. This is in good agreement with previous results of Suvorov et al. [15], who detected Al precipitates with sizes up to 40 nm in 6H-SiC after high temperature (1400–1600 °C) implantation of Al with a peak concentration of about $2 \times 10^{20} \text{ cm}^{-3}$ and subsequent annealing at 1800 °C for 5 s.

A supersaturation of Al in crystalline SiC can be attained by high dose implantation at moderate temperatures. The critical Al concentration below that no precipitation has been observed in the as-implanted state is about $1 \times 10^{22} \text{ cm}^{-3}$ (10 at.%) for implantation at 500 °C [7]. Above this critical Al concentration, Al_4C_3 and Si precipitates, which are epitaxially embedded in the 6H-SiC matrix, are formed. At higher implantation temperatures the growth of Al precipitates is favored against the Al_4C_3 formation [16]. High temperature annealing of these heterogeneous layers leads to further decomposition of the SiC matrix. Al precipitates and cavities with sizes ranging from 10 to 500 nm have been detected in a highly defected SiC matrix after annealing at 1400 °C [17]. Consequently, device grade, single crystalline SiC with Al concentrations above $1 \times 10^{22} \text{ cm}^{-3}$ cannot be produced. The furnace annealing of SiC samples with subcritical Al concentrations (1–5 at.%) leads to Al precipitation, too. However, no cavities are formed and less lattice defects are present because of the smaller size (5–20 nm) of the epitaxial Al precipitates.

4. Damage generation and annealing

The key problem of high dose ion implantation is the formation of radiation damage which is very stable in SiC [18] and has to be annealed out in order to obtain high acceptor activation and hole mobility. The damage accumulation during RT implantation leads to amorphization. The critical damage energy is about $2 \times 10^{24} \text{ eV cm}^{-3}$ if the ion energy is below 500 keV [19]. A higher critical damage energy of $5.6 \times 10^{24} \text{ eV cm}^{-3}$ has been found for MeV implantation [20]. In the case of box-like Al profiles which are produced by multiple energy implantation the amorphization energy at RT roughly corresponds to an Al plateau concentration of about $2 \times 10^{19} \text{ cm}^{-3}$ or a total dose of $1 \times 10^{15} \text{ cm}^{-2}$ for a typical layer width of 500 nm. However, the amorphization dose is a strong function of the target temperature in the range

between RT and 200 °C [20,21]. Thus, the amorphization can remain incomplete even for doses which are supercritical at RT if unintentional beam heating effects raise the target temperature during implantation at nominal RT.

Unfortunately, most of the attempts to stimulate complete epitaxial regrowth of amorphous layers on crystalline SiC substrates have failed until now. It has been demonstrated that the amorphous phase starts to recrystallize at temperatures above 700 °C [23]. The nucleation and growth of 3C–SiC grains in the amorphous matrix is the dominating process [24]. Crystallization temperatures below 700 °C that have sometimes been reported [25] are likely due to incomplete layer amorphization.

With increasing annealing temperatures the recrystallization mode switches from random nucleation to layer by layer growth, which is disturbed by twinning, the partial transformation to the 3C polytype and the formation of stacking faults [26]. Even annealing at 1700 °C cannot transform the amorphous SiC layers to device grade material. Previous results on apparent explosive solid phase epitaxy (SPE) at 1450 °C [27] can be explained by chemical layer etching due to an oxygen or water polluted annealing atmosphere [18]. Recrystallization can be stimulated by ion irradiation at temperatures as low as 300 °C. However, also in this case no complete epitaxial regrowth can be obtained. Instead, the random nucleation is strongly enhanced [28]. Ottaviani et al. [29] reported about complete epitaxial regrowth of Al doped 6H–SiC layers, 500 nm thick with an Al concentration of $4 \times 10^{19} \text{ cm}^{-3}$ (twice the critical one for amorphization) produced by implantation at RT. The annealing was performed at 1700 °C for 30 min. It can be speculated that the very high heating rate (up to 60 K/s) which was applied could prevent disturbing nucleation. However, recent annealing experiments carried out at similar conditions on SiC samples implanted with a higher Al dose (plateau concentration $5 \times 10^{20} \text{ cm}^{-3}$) did not confirm this idea. According to Satoh et al. [30] the bad quality regrowth obtained for standard SiC material is due to its (0 0 0 1) orientation which is indefinite with regard to the polytype structure. Consequently, stacking faults can easily be produced during the SPE regrowth. Almost perfect SPE has been observed on (1–100) oriented 4H– and 6H–SiC amorphized by Al

and Ga implantation and subsequently annealed at 1500 °C for 30 min [31].

Because of the serious problems associated with the annealing of amorphous layers on SiC with the standard (0 0 0 1) orientation, most of the doping implantations have been carried out at elevated temperatures. Amorphization is completely avoided if the implantation temperature exceeds a critical value that depends on the damage energy and the dose rate [22]. For Al implantation, this critical temperature is in the range between 170 and 250 °C. The influence of the implantation temperature on the resistivity of 6H–SiC doped with $5 \times 10^{19} \text{ cm}^{-3}$ Al has been investigated in the temperature range between RT and 1200 °C [32]. In the as-implanted state, a weak p-type conductivity has only been observed for the highest implantation temperature. The application of even higher implantation temperatures for a direct acceptor activation is complicated by technical problems and not beneficial because enhanced surface erosion leads to an increased surface roughness and Al losses. After annealing at 1650 °C for 10 min the lowest resistivity was measured at the sample implanted at 400 °C. Very likely, the lower conductivity obtained for the samples implanted at higher temperatures is due to the enhanced formation of dislocation loops as proved by XTEM studies. It can be supposed that the competition between disorder production at lower temperatures and the formation of secondary defects at higher temperatures determines the optimum implantation temperature. To our experience, implantation temperatures above 600 °C do not facilitate the post-implantation activation of Al in SiC by annealing. Moreover, it seems that Al implantations with doses below the amorphization threshold can be performed even at RT without any deterioration of the activation behavior [1,12].

At the present stage furnaces [29] or CVD reactors [38] with inductively heated graphite susceptor are mainly used for post-implantation annealing. Typically, the SiC samples are annealed in SiC coated graphite boxes under Ar atmosphere. The influence of the annealing temperature on the Al activation has been investigated by several groups [1,33–35]. Best activation results have been obtained for annealing temperatures between 1600 and 1700 °C. The annealing time has only a weak influence on the Al activation at such high temperatures and typically ranges from 10

to 45 min. However, long-term furnace annealing at temperatures above 1600 °C can cause surface degradation by Si sublimation. Surface erosion and roughening is a quite general problem of high temperature annealing [35]. Surface capping and the optimization of the annealing ambient have been proposed as appropriate precautions. It has been shown that graphite [36] and AlN [37] encapsulation can protect the surface up to annealing temperatures of 1660 and 1600 °C, respectively. In order to prevent Si sublimation, there have been several attempts to increase the Si partial pressure by the addition of Si (powder or pieces) in the annealing crucible or by using a mixture of SiH₄ and Ar as annealing atmosphere [38].

Because of the problems of long-term furnace annealing flash lamp annealing has been investigated as an alternative activation process. Wirth et al. [33] used an array of xenon lamps with a flash duration of 20 ms that provides energy densities of 100–150 J cm⁻². Since the light absorption coefficient of crystalline SiC is very low, the wafer backside was amorphized by ion implantation and preheated by halogen lamps up to temperatures of 700 °C. The high thermal conductivity of SiC ensures a rapid temperature equilibration over the whole wafer thickness. The maximum temperature obtained in this annealing process is about 2000 °C. In comparison

with conventional furnace annealing, the free hole concentration can be enhanced for Al concentrations $\geq 5 \times 10^{20}$ cm⁻³ [33,34,39]. However, at such high Al concentrations the normal band conductivity is lost and a metallic-like carrier transport has been observed by Hall measurements. At lower Al concentrations the flash lamp annealing could not produce better Al activation than furnace annealing. Nevertheless, it is well suited for efficient high temperature annealing of large area wafers due to short annealing cycles and low thermal budget. In particular, surface etching and dopant out-diffusion can be reduced by this technique.

5. Summary and conclusions

The Al acceptor is best-suited for the production of low resistivity p-type SiC because it has the lowest ionization energy in SiC and a natural tendency to occupy electrically active Si sites. A further advantage is its high solubility which reduces the problems associated with acceptor losses by precipitation as known from B doping. However, also in the ideal case of uncompensated and fully activated acceptors, the RT resistivity cannot be brought below 0.05 Ω cm in heavily Al doped SiC as long as normal, thermally stimulated band conduction is the dominating process.

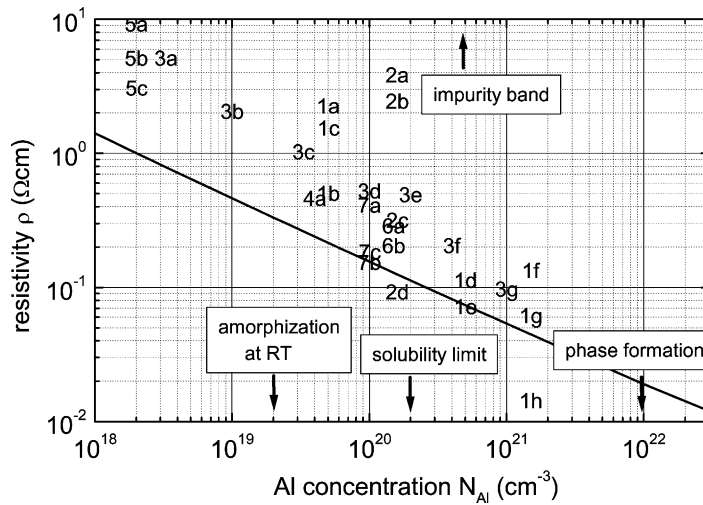


Fig. 4. Comparison of experimental results for the resistivity of p-type SiC produced by Al implantation and subsequent annealing with the predicted minimum resistivity (solid line). The process parameters and references are given in Table 3. The critical concentrations for amorphization at RT implantation, the onset of precipitation at elevated temperatures, impurity band formation and phase formation are indicated.

Table 3
Process parameters of selected doping experiments for the production of low resistivity p-type SiC

No./Ref.	Layer width (nm)	Al concentration (cm^{-3})	Implantation temperature ($^{\circ}\text{C}$)	Annealing temperature/time ($^{\circ}\text{C}/\text{min}$)	Resistivity ($\Omega \text{ cm}$)	Substrate/comments
1a/[33]	500	5×10^{19}	400	1550/10	2.2	6H
1b/[33]	500	5×10^{19}	400	1650/10	0.49	6H
1c/[33]	500	5×10^{19}	400	2000/20 ms	1.5	6H, flash lamp annealing
1d/[33]	500	5×10^{20}	400	1650/10 min	0.11	6H
1e/[33]	500	5×10^{20}	400	2000/20 ms	0.07	6H, flash annealing, metallic conduction
1f/[33]	500	1.5×10^{21}	400	1550/10	0.13	6H
1g/[33]	500	1.5×10^{21}	400	1650/10	0.060	6H
1h/[33]	500	1.5×10^{21}	400	2000/20 ms	0.014	6H, flash annealing, metallic conduction
2a/[40]	250	1.6×10^{20}	RT	1600	3.75	4H (11–20)
2b/[40]	250	1.6×10^{20}	RT	1700	2.38	4H (11–20)
2c/[40]	250	1.6×10^{20}	500	1600	0.31	4H (11–20)
2d/[40]	250	1.6×10^{20}	500	1700	0.090	4H (11–20)
3a/[11]	240	3.3×10^{18}	650	1670/6–12	5	4H
3b/[11]	240	1×10^{19}	650	1670/6–12	2	4H
3c/[11]	240	3.3×10^{19}	650	1670/6–12	1	4H
3d/[11]	240	1×10^{20}	650	1670/6–12	0.51	4H
3e/[11]	240	2×10^{20}	650	1670/6–12	0.48	4H
3f/[11]	240	4×10^{20}	650	1670/6–12	0.2	4H
3g/[11]	240	1×10^{21}	650	1670/6–12	0.095	4H
4a/[29]	450	4×10^{19}	RT	1700/30	0.45	6H, rapid heating $> 40^{\circ}\text{K}/\text{s}$
5a/[1]	1600	2×10^{18}	500	1600/30	9	4H
5b/[1]	1600	2×10^{18}	500	1700/30	5	4H
5c/[1]	1600	2×10^{18}	500	1800/30	3	4H
6a/[37]	200	1.5×10^{20}	800	1600/15	0.28	6H, AlN cap
6b/[37]	200	1.5×10^{20}	800	1600/30	0.20	6H, AlN cap
7a/[8]	270	1×10^{20}	850	1600/45	0.4	6H,
7b/[8]	270	1×10^{20}	850	1600/45	0.15	6H, C co-implantation, $1 \times 10^{20} \text{ cm}^{-3}$
7c/[8]	270	1×10^{20}	850	1600/45	0.18	6H, C co-implantation, $5 \times 10^{20} \text{ cm}^{-3}$

This limit is settled by the physical constraints for the acceptor ionization and hole mobility under the conditions of high Al concentrations. The very upper concentration where normal band conduction has been observed is $1 \times 10^{21} \text{ cm}^{-3}$ Al (1 at.%). However, for fully activated Al acceptors the Mott transition to impurity band, metallic-like conduction can be predicted for $2 \times 10^{20} \text{ cm}^{-3}$ Al. Nevertheless, Al impurity band conduction can be exploited for the formation of low resistivity contact areas to p-type material.

Typically, the efficiency of doping has been assessed on the basis of the acceptor activation grade determined from the temperature dependence of the hole concentration. Unfortunately, the temperature range over which Hall measurements have to be carried out for a reliable analysis of the acceptor activation is much too high for heavily Al doped SiC. Therefore, many of the activation data given in the literature appear rather doubtful. In order to assess the quality of the doping it is better to directly compare hole concentrations and resistivities for a given Al concentration. In Fig. 4, some resistivity results obtained after Al implantation and subsequent annealing are presented along with the rough estimation of the theoretical limit of the resistivity. The parameters of the doping processes are presented in Table 3. As it can be seen, some of the results are very close to the theoretical limit indicating optimal doping conditions.

The following general conclusions for efficient p-type doping by Al implantation can be drawn. For the mostly used (0 0 0 1) oriented SiC amorphization must be avoided by implantation at elevated temperatures because perfect epitaxial regrowth is not possible. The optimum temperature range for implantation is between 400 and 600 °C. Higher implantation temperatures can deteriorate the electrical properties by the formation of secondary defects. C co-implantation can help to activate the acceptors if the Al concentration is below $1 \times 10^{20} \text{ cm}^{-3}$. Furnace annealing at temperatures between 1600 and 1700 °C yields the best activation results for Al doping with concentrations up to $5 \times 10^{20} \text{ cm}^{-3}$. At higher Al concentrations flash lamp annealing (20 ms, 2000 °C) is the superior process.

References

- [1] T. Troffer, M. Schadt, T. Frank, H. Itoh, G. Pensl, J. Heindl, H.P. Strunk, M. Maier, *Phys. Stat. Sol. (a)* 162 (1997) 277.
- [2] M. Ruff, H. Mittlehner, R. Helbig, *IEEE Trans. Electron. Dev.* 41 (1994) 1040.
- [3] W.J. Schaffer, G.H. Negley, K.G. Irvine, J.W. Palmour, *Mater. Res. Soc. Symp. Proc.* 339 (1994) 595.
- [4] A. Schöner, N. Nordell, K. Rottner, R. Helbig, *G. Pensl, Inst. Phys. Conf. Ser.* 142 (1995) 493.
- [5] A. Schroeder, R. Pelster, V. Grunov, W. Lennartz, G. Nimitz, K. Friedrich, *J. Appl. Phys.* 80 (1996) 2260.
- [6] V.A. Gubanov, C.Y. Fong, *Appl. Phys. Lett.* 75 (1999) 88.
- [7] V. Heera, H. Reuther, J. Stoemenos, B. Pécz, *J. Appl. Phys.* 87 (2000) 78.
- [8] M.V. Rao, P. Griffiths, J. Gardner, O.W. Holland, M. Ghezzi, J.A. Kretchmer, G. Kelner, J.A. Freitas, *J. Electron. Mater.* 25 (1996) 75.
- [9] H. Itoh, T. Troffer, *G. Pensl, Mater. Sci. For.* 264–268 (1998) 685.
- [10] K. Tone, J.H. Zhao, *IEEE Trans. Electron. Dev.* 46 (1999) 612.
- [11] J.M. Bluet, J. Pernot, T. Billon, S. Contreras, J.F. Michaud, J.L. Robert, J. Camassel, *Mater. Sci. For.* 338–342 (2000) 887.
- [12] T. Ohshima, H. Itoh, M. Yoshikawa, *Mater. Sci. For.* 353–356 (2001) 575.
- [13] Y.A. Vodakov, E.N. Mokhov, M.G. Ramm, A.D. Roenkov, *Springer Proc. Phys.* 56 (1992) 329.
- [14] M.K. Linnarson, P.O.A. Person, H. Bleichner, M.S. Janson, U. Zimmerman, H. Andersson, S. Karlsson, R. Yakimova, L. Hultmann, B.G. Svensson, *Mater. Sci. For.* 353–356 (2001) 583.
- [15] A.V. Suvorov, O.I. Lebedev, A.A. Suvorova, J. Van Landuyt, I.O. Usov, *Nucl. Instrum. Meth. B* 127–128 (1997) 347.
- [16] V. Heera, W. Skorupa, J. Stoemenos, B. Pécz, *Mater. Sci. For.* 353–356 (2001) 579.
- [17] J. Stoemenos, B. Pécz, V. Heera, *Mater. Sci. For.* 338–342 (2000) 881.
- [18] V. Heera, W. Skorupa, *Mater. Res. Soc. Symp. Proc.* 438 (1997) 241.
- [19] J.A. Spitznagel, S. Wood, W.J. Choyke, N.J. Doyle, J. Bradshaw, S.G. Fishman, *Nucl. Instrum. Meth. B* 16 (1986) 327.
- [20] T. Henkel, V. Heera, R. Kögler, W. Skorupa, *J. Appl. Phys.* 84 (1998) 3090.
- [21] A. Heft, E. Wendler, J. Heindl, T. Bachmann, E. Glaser, H.P. Strunk, W. Wesch, *Nucl. Instrum. Meth. B* 113 (1996) 239.
- [22] E. Wendler, A. Heft, W. Wesch, *Nucl. Instrum. Meth. B* 141 (1998) 105.
- [23] A. Höfgen, V. Heera, F. Eichhorn, W. Skorupa, *J. Appl. Phys.* 84 (1998) 4769.
- [24] J. Pezoldt, A.A. Kalnin, D.R. Moskwin, W.D. Savelyev, *Nucl. Instrum. Meth. B* 80–81 (1993) 943.
- [25] W. Jiang, W.J. Weber, S. Thevuthasan, D.E. McCready, *Nucl. Instrum. Meth. B* 143 (1998) 333.
- [26] S. Harada, M. Ishimaru, T. Mottoka, *Appl. Phys. Lett.* 69 (1996) 3534.
- [27] C.J. McHargue, J.M. Williams, *Nucl. Instrum. Meth. B* 80–81 (1993) 889.
- [28] V. Heera, J. Stoemenos, R. Kögler, M. Voelskow, W. Skorupa, *J. Appl. Phys.* 85 (1999) 1378.

- [29] L. Ottaviani, E. Morvan, M.L. Locatelli, D. Planson, P. Godignon, J.P. Chante, A. Senes, *Solid State Electron.* 43 (1999) 2215.
- [30] M. Satoh, K. Okamoto, Y. Nakaike, K. Kuriyama, M. Kanaya, N. Ohtani, *Nucl. Instrum. Meth. B* 148 (1999) 567.
- [31] M. Satoh, Y. Nakeike, K. Uchimura, K. Kuriyama, *Mater. Sci. For.* 338–342 (2001) 905.
- [32] D. Panknin, H. Wirth, A. Mücklich, W. Skorupa, *Mater. Sci. Eng. B* 61–62 (1999) 363.
- [33] H. Wirth, D. Panknin, W. Skorupa, E. Niemann, *Appl. Phys. Lett.* 74 (1999) 979.
- [34] D. Panknin, T. Gebel, W. Skorupa, *Mater. Sci. For.* 353–356 (2001) 587.
- [35] M.A. Capano, *Mater. Res. Soc. Symp. Proc.* 640, in press.
- [36] Ch. Thomas, C. Taylor, J. Griffin, W.L. Rose, M.G. Spencer, M. Capano, S. Rendakova, K. Kornegay, *Mater. Res. Soc. Symp. Proc.* 572 (1999) 45.
- [37] E.M. Handy, M.V. Rao, K.A. Jones, M.A. Derenge, P.H. Chi, R.D. Vispute, T. Venkatesan, N.A. Papanicolaou, J. Mittereder, *J. Appl. Phys.* 86 (1999) 746.
- [38] S.E. Sadow, J. Williams, T. Isaacs-Smith, M.A. Capano, J.A. Cooper, M.S. Mazzola, A.J. Hsieh, J.B. Casady, *Mater. Sci. For.* 338–342 (2000) 901.
- [39] D. Panknin, H. Wirth, W. Anwand, G. Brauer, W. Skorupa, *Mater. Sci. For.* 338–342 (2000) 877.
- [40] T. Kimoto, H. Yano, S. Tamura, N. Miyamoto, K. Fujihira, Y. Negoro, H. Matsunami, *Mater. Sci. For.* 353–356 (2001) 543.